Integral Sliding Mode Controller for Magnetically Suspended Balance Beam : Theory and Experimental Evaluation

Jun-Ho Lee†, Edgar F. Hilton†, Xuerui Zhang‡, Gang Tao‡, Paul E. Allaire†

† Department of Mechanical and Aerospace Engineering, University of Virginia, Charlottesville, Virginia, 22903 USA. E-mail:jl7e@virginia.edu, efh4v@virginia.edu, pea@virginia.edu, respectively

‡ Department of Electrical Engineering, University of Virginia, Charlottesville, Virginia, 22903 USA. E-mail:xz5d@virginia.edu, gt9s@ral.ee.virginia.edu, respectively

ABSTRACT

This paper deals with a sliding mode controller with integral compensation in a magnetic suspension system. The control scheme comprises an integral controller which is designed for achieving zero steady-state error under step disturbance input, and a sliding mode controller which is designed for enhancing robustness under plant parametric variations. A procedure is developed for determining the coefficients of the switching plane and integral control gain such that the overall closed-loop system has stable eigenvalues. A proper continuous design signal is introduced to overcome the chattering problem. The performance of a magnetically suspended balance beam using the proposed integral sliding mode controller is illustrated. Simulation and experimental results show that the proposed method is effective under the external step disturbance and input channel parameter variations.

INTRODUCTION

Electromagnetic bearings inherently have nonlinear properties [2]. With regard to such a nonlinear system, various controllers have been developed. The integral sliding mode control approach has been reported by a number of authors recently as a method of servo control [1],[6],[7]. The integral sliding mode control approach consists of two compensators: one uses an integral compensator for achieving a zero steady-state error under an external step disturbance force, and the other uses a sliding mode controller. Sliding mode controllers select a surface in phase space, typically a linear hypersurface, called the switching surface, and switch the control input on this surface. The control input is then chosen to guarantee that trajectories near the sliding surface are directed toward the surface via reaching conditions. Once the system is on the surface, the system closed-loop dynamics are completely governed by the equations which define the surface. The closed-loop dynamics will be insensitive to the parameter variations of the input channel and robustness is achieved [3],[4],[5].

The design problem of an integral sliding mode controller consists of three items. The first item is concerned with the design of a switching surface σ upon which desired dynamic behavior can be guaranteed for

the nominal system. The second item is concerned with the selection of a proper nonlinear control law to handle strong nonlinearities of the initial states of the magnetically suspended system. The third item is to select a proper integrator gain.

In this paper we apply an integral sliding mode control method to a magnetically suspended balance beam to achieve zero steady-state error under an external step disturbance and it's insensitivity with respect to the parametric variations of the input channel. We first derive the linearized mathematical model with integrator of the magnetically suspended balance beam at the nominal point, and then construct the integral sliding mode controller using a pole placement method to a designed switching surface. Simulation and experimental results show that an integral sliding mode control design can achieve accurate tracking and is fairly robust to plant parameter variations and external load disturbances.

MATHEMATICAL MODEL

Fig. 1 shows the geometry of the symmetric balance beam with two magnetic bearings, and Table 1 shows each parameter of the balance beam. The balance beam shown in fig. 1 can be modeled by using

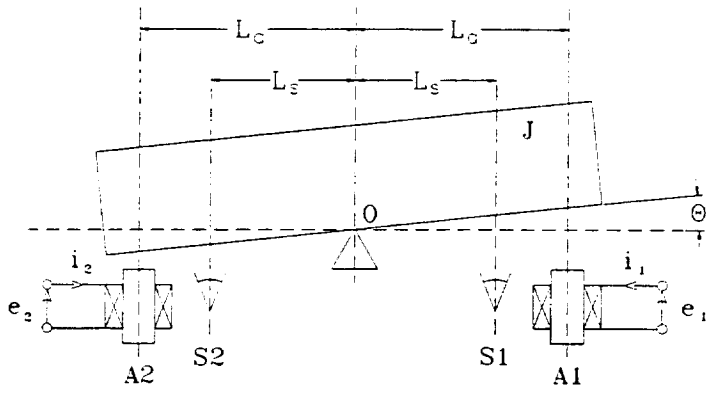

Figure 1: Symmetric balance beam on two magnetic bearings.

Table 1: Balance Beam Parameters

Parameter	Symbol	Value	Units
Angular Position	θ		rad
Half Bearing Span	L_a	1.1412	m
Mass Moment of Inertia about the Pivot Point	J	0.0948	kg/m^2
Coil Current in Bearing 1	i_1		A
Coil Current in Bearing 2	i_2		A
Control Voltage in Bearing 1	e_1		V
Control Voltage in Bearing 2	e_1		V
Coil Resistance	R	0.7	Ω
Coli Inductance	L	0.545	mH
Magnetic Bearing Open Loop Stiffness	K_x	2114	N/m
Actuator Current Gain	K_i	1.074	N/A
Steady Current	I	1	A
Steady Gap	G	380	μm

the second order dynamic equation and voltage equation.

$$J\ddot{\theta} = L_a(f_1 - f_2) + f_d \tag{1}$$

$$e' = Ri' + L\frac{di'}{dt} \tag{2}$$

where J is the mass moment of inertia about the pivot point, L_a is the half bearing span, f_1 is the electromagnetic attractive force in bearing 1, f_2 is the electromagnetic attractive force in bearing 2, f_d is the external disturbance force, R is the coil resistance, L is the coil inductance, $e' = e_1 - e_2$ is the control voltage difference, and $i' = i_1 - i_2$ is the instantaneous coil current difference. Eqs. (1) and (2) can be linearized by a Taylor series expansion about the operating point, $\theta = 0$, $e' = 0$, $i' = 0$. Eq. (3) shows the linearized state space equations of the balance beam.

$$\begin{aligned} \dot{x} &= Ax + Bu + f_d \\ y &= Cx \end{aligned} \tag{3}$$

where,

$$x = \begin{bmatrix} \theta \\ \dot{\theta} \\ i' \end{bmatrix}, \quad A = \begin{bmatrix} 0 & 1 & 0 \\ \frac{2K_x L_a^2}{J} & 0 & \frac{K_i L_a}{J} \\ 0 & -2K_i\frac{1}{L} & -\frac{R}{L} \end{bmatrix}, \quad B = \begin{bmatrix} 0 \\ 0 \\ \frac{1}{L} \end{bmatrix}$$
$$C = \begin{bmatrix} 1 & 0 & 0 \\ 0 & 1 & 0 \\ 0 & 0 & 1 \end{bmatrix}, \quad u = e' \tag{4}$$

In order to include the integrator as a state variable into (3), we design the following block diagram shown

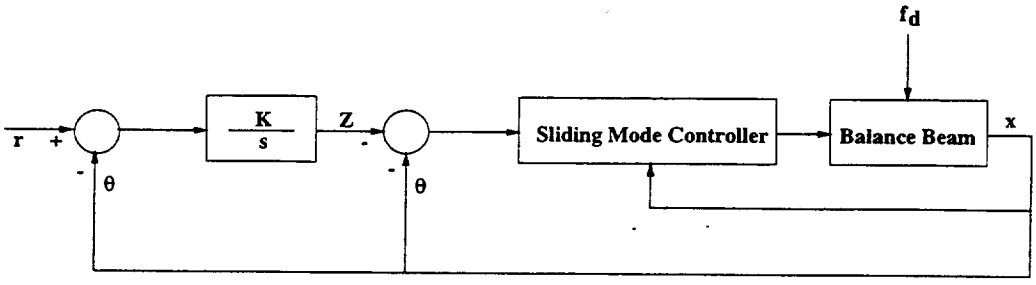

Figure 2: Block diagram of an integral-sliding-mode-controlled balance beam

in fig. 2. Here the integrator output Z is expressed as the difference between the integrated reference angular position r and integrated angular position θ written as:

$$Z = \int (r - \theta)dt \tag{5}$$

where $r = 0$. By using (5) we construct new state space equations including the integrator as a state variable.

CONTROLLER SYNTHESIS

In order to synthesize the integral sliding mode controller we write the state variables as $x = [Z \ \theta \ \dot{\theta} \ i']^T$, and get the following state space matrices.

$$A = \begin{bmatrix} 0 & -1 & 0 & 0 \\ 0 & 0 & 1 & 0 \\ 0 & \frac{2K_s L_a^2}{J} & 0 & \frac{K_i L_a}{J} \\ 0 & 0 & -2K_i \frac{1}{L} & -\frac{R}{L} \end{bmatrix}, \quad B = \begin{bmatrix} 0 \\ 0 \\ 0 \\ \frac{1}{L} \end{bmatrix}, \quad C = \begin{bmatrix} 0 & 0 & 0 & 0 \\ 0 & 1 & 0 & 0 \\ 0 & 0 & 1 & 0 \\ 0 & 0 & 0 & 1 \end{bmatrix} \tag{6}$$

Here, we can formulate the sliding mode state space equations by decomposing (6) such as:

$$\begin{bmatrix} \dot{x}_1 \\ \dot{x}_2 \end{bmatrix} = \begin{bmatrix} A_{11} & A_{12} \\ A_{21} & A_{22} \end{bmatrix} \begin{bmatrix} x_1 \\ x_2 \end{bmatrix} + \begin{bmatrix} B_1 \\ B_2 \end{bmatrix} u \tag{7}$$

where,

$$x_1 = \begin{bmatrix} Z \\ \theta \\ \dot{\theta} \end{bmatrix}, \quad x_2 = i'$$

$$A_{11} = \begin{bmatrix} 0 & -1 & 0 \\ 0 & 0 & 1 \\ 0 & \frac{2K_s L_a^2}{J} & 0 \end{bmatrix}, \quad A_{12} = \begin{bmatrix} 0 \\ 0 \\ \frac{K_i L_a}{J} \end{bmatrix}, \quad A_{21} = \begin{bmatrix} 0 & 0 & -2K_i \frac{1}{L} \end{bmatrix}, \quad A_{22} = -\frac{R}{L}$$

$$B_1 = \begin{bmatrix} 0 \\ 0 \\ 0 \end{bmatrix}, \quad B_2 = \frac{1}{L}, \quad u = e' \tag{8}$$

Let the sliding mode surface be defined as $\sigma = Sx$.

$$\sigma = \begin{bmatrix} S_1 & S_2 \end{bmatrix} \begin{bmatrix} x_1 \\ x_2 \end{bmatrix} \tag{9}$$

If the system dynamics yield ideal sliding mode dynamics (9) equals zero or $\sigma = Sx = 0$. By using this property we can determine the equivalent linear control input from (9). x_2 becomes

$$x_2 = \frac{\sigma - S_1 x_1}{S_2} \tag{10}$$

Substituting (10) into (7) yields

$$\dot{x}_1 = (A_{11} - A_{12} S_2^{-1} S_1) x_1 + A_{12} S_2^{-1} \sigma \tag{11}$$

The sliding surface is defined as $\sigma = S_1 x_1 + S_2 x_2 = 0$. Eq. (11) becomes

$$\dot{x}_1 = (A_{11} - A_{12} S_2^{-1} S_1) x_1 = (A_{11} - A_{12} k) x_1 \tag{12}$$

where $k = S_2^{-1} S_1$. The location of poles of the sliding mode surface are obtained by selecting k. The equation for the sliding surface becomes $S = [S_1 \ \ S_2] = [S_2 k \ \ S_2] = S_2 [k \ \ 1]$.

The sliding mode control input can be separated into the linear and nonlinear components as $u = u_l + u_{nl}$. The linear input can be selected by the following equations:

$$\dot{x} = Ax + Bu \tag{13}$$

$$\dot{\sigma} = S\dot{x} = 0 \tag{14}$$

From eq. (13), (14) we can get the equivalent linear control input as:

$$u = u_l = -(SB)^{-1}SAx \tag{15}$$

The sliding mode reaching condition, given by $\sigma\dot{\sigma} < 0$, brings the balance beam to the sliding surface. If the nonlinear control is given by $u_{nl} = -(SB)^{-1}\rho sgn(\sigma)$ where $\rho > 0$, $(SB)^{-1} = I$. The reaching condition becomes

$$\sigma\dot{\sigma} = -\rho\sigma sgn(\sigma) < 0 \tag{16}$$

The control input can then be written as

$$u = -(SB)^{-1}[SAx + \rho sgn(\sigma)] \tag{17}$$

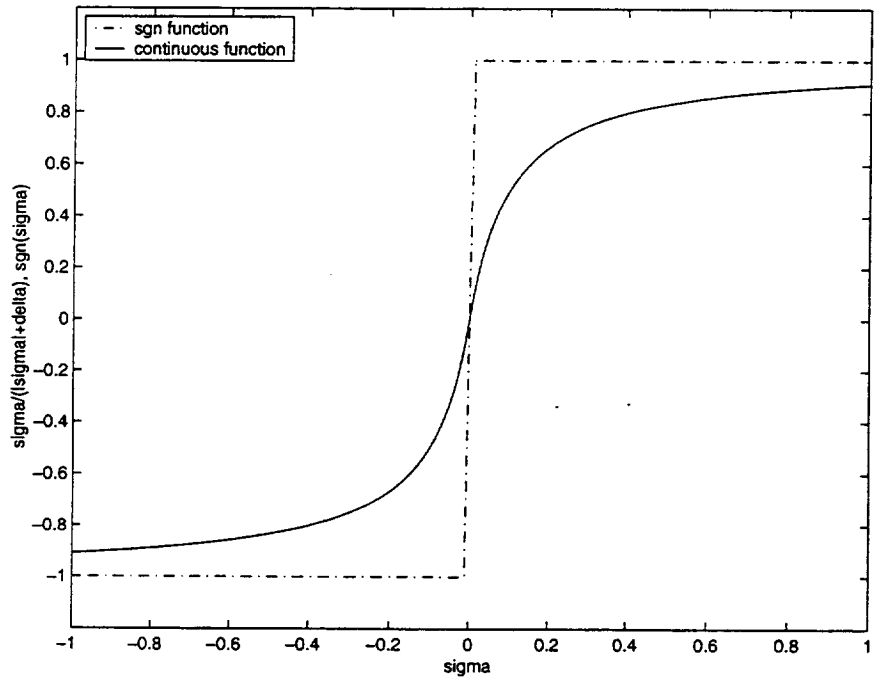

Figure 3: Sliding surface using discontinuous and continuous function

In practical terms such a nonlinear discontinuous control component is undesirable because the $sgn(\sigma)$

function may cause a chattering problem. So, the control effort is required to ensure σ or a neighborhood of σ is reached and maintained. Ideally, a control strategy is required to ensure that the system dynamics is both close to σ and as close as possible to the ideal sliding mode dynamics. With this point of view, modern design methods employ a continuous, usually nonlinear, control to ensure system dynamics within a region containing σ. Let the nonlinear control input be defined as the continuous function

$$u_{nl} = -\rho \frac{\sigma}{|\sigma| + \delta} \tag{18}$$

where δ is the boundary layer which is selected to reduce the chattering problem and ρ is a design parameter. Fig. 3 shows the relation between the discontinuous *sgn* function and continuous function. In this figure we can see that the slope of the continuous function depends upon δ. Fig. 4 shows the block diagram of the designed sliding mode controller connected to the integral compensator.

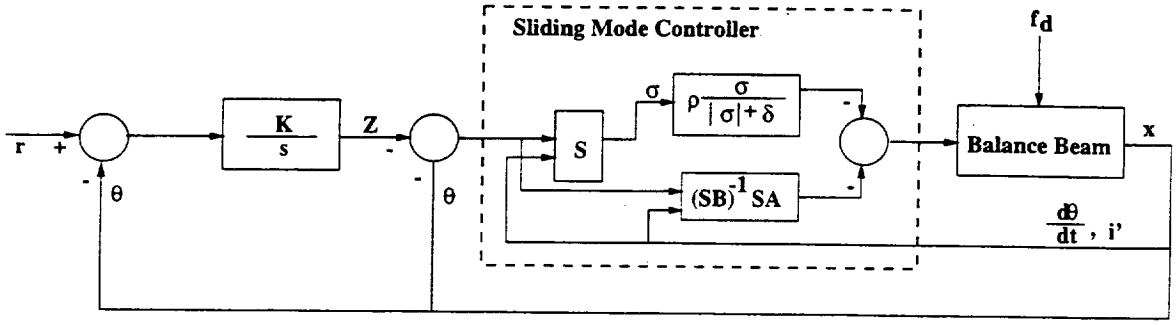

Figure 4: Block diagram of integral sliding mode control implementation

SIMULATION RESULTS

In order to show the effectiveness of the proposed controller we consider a comparison between the integral sliding mode controller and a simple integral state feedback controller. For making the parameter variations, we changed the nominal inductance value($L = 7.2727 \times 10^{-4}$[H]) was changed from $0.1L$ to $10L$, where the nominal inductance is a function of nominal gap. The vector S which defines the sliding surface, design parameters of the nonlinear control components and linear component gain matrices $Fl = (SB)^{-1}SA$ are such as:

1. When the nominal inductance is applied($x = [Z \ \ \theta \ \ \dot{\theta} \ \ i']^T$)

$$\begin{aligned} S &= [3.5174508 \times 10^5 \ \ 9886.579 \ \ 91.453 \ \ 1.0] \\ Fl &= [0 \ \ 395.9667 \ \ 6.6511 \ \ -0.5109] \\ \rho &= 10, \ \delta = 0.4 \end{aligned} \tag{19}$$

2. When 10 times of the nominal inductance is applied($x = [Z \ \ \theta \ \ \dot{\theta} \ \ i']^T$)

$$\begin{aligned} S &= [3.5174508 \times 10^5 \ \ 9886.579 \ \ 91.453 \ \ 1.0] \\ Fl &= [0 \ \ 3959.666 \ \ 71.362 \ \ 1.190] \\ \rho &= 10, \ \delta = 0.4 \end{aligned} \tag{20}$$

3. When 0.1 times of the nominal inductance is applied($x = [Z \ \theta \ \dot{\theta} \ i']^T$)

$$S = [3.5174508 \times 10^5 \ \ 9886.579 \ \ 91.453 \ \ 1.0]$$
$$Fl = [0 \ \ 39.5967 \ \ 0.1800 \ \ -0.6811]$$
$$\rho = 10, \ \delta = 0.4 \tag{21}$$

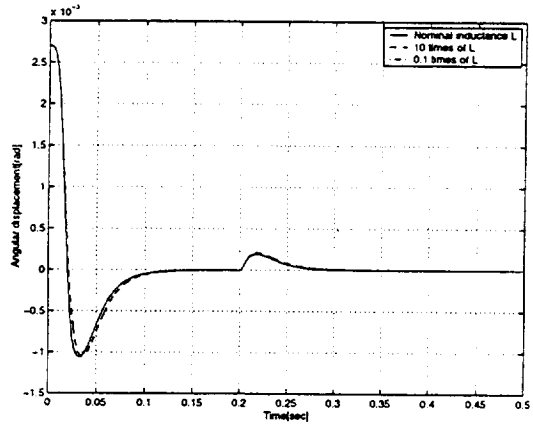

Figure 5: Evolution of angular displacement by integral sliding mode controller

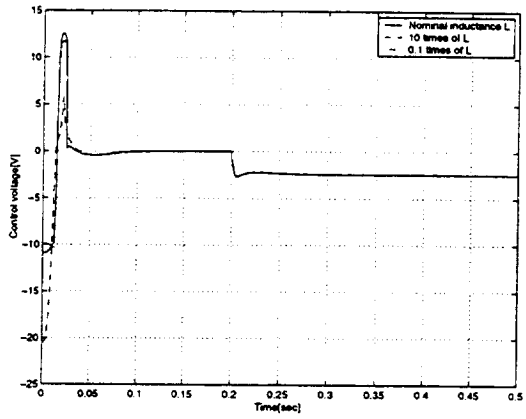

Figure 6: Evolution of control effort by integral sliding mode controller

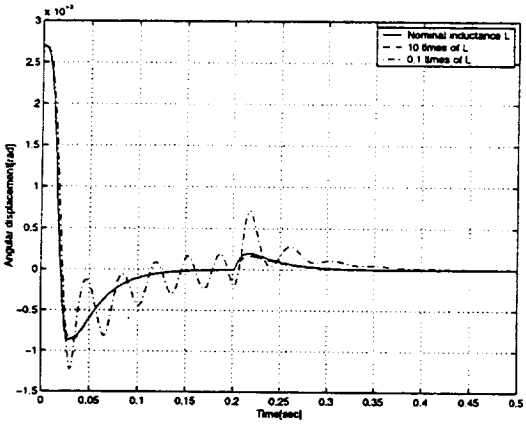

Figure 7: Evolution of angular displacement by integral state feedback controller

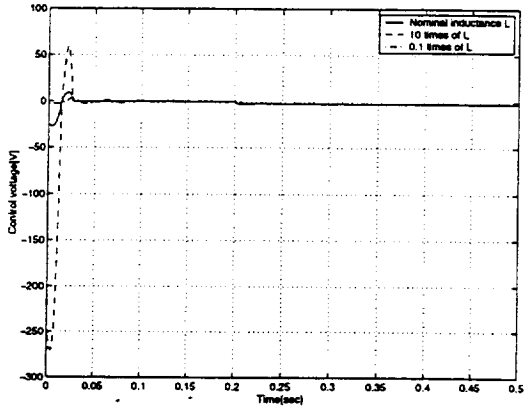

Figure 8: Evolution of control effort by integral state feedback controller

Fig. 5 - 8 show the simulation results under the parameter variations and the external step disturbance(0.2sec 1[N]). In fig. 5 the angular displacements are in close agreement, thereby illustrating the insensitivity to parameter variations. However fig. 6 shows significant difference in control effort. In fig. 7, 8 we can see the significant angular displacements and significant overshoot in control voltage which is controlled by the simple integral state feedback controller. This means that our proposed integral sliding mode controller is very robust over the parameter variations and external step disturbances.

EXPERIMENTAL SETUP

Fig. 9 shows the total experimental setup. Near the magnetic bearings of the balance beam there are two eddy-current type displacement sensors. The experimental machine is controlled by a digital control system **that consists of 450 MHz Intel Pentium II Processor which is loaded with Real Time Linux OS (version Beta 16) running Real Time Control Laboratory (http://www.people.virginia.edu/~efh4v) [8], 12 bits A/D and D/A converters, LPF which has 1.2 kHz cutoff frequency. In our amplifier we use an H-bridge (4 HEXFETS, International Rectifier Co.) This amplifier operates on 20 kHz (much higher than the natural frequency of the balance beam) and ±15 V power supply voltage.**

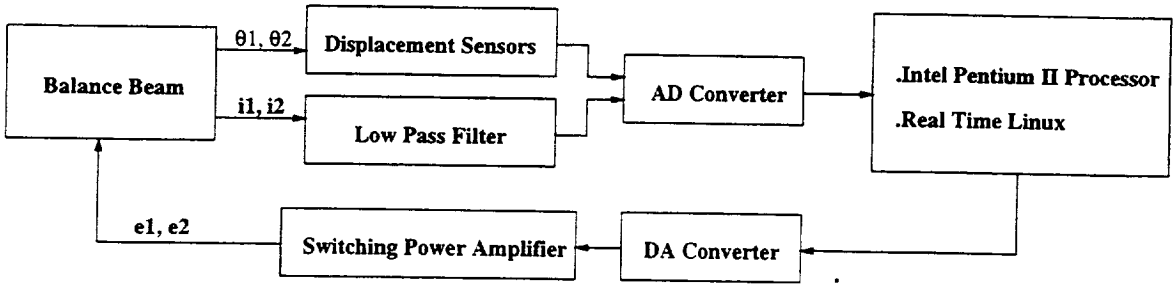

Figure 9: Block diagram of experimental setup

EXPERIMENTAL RESULTS

Fig. 10 - 15 show the gap deviations under the parametric variations and external load disturbance. In order to make the parametric variations the nominal inductance was changed from $2L$ to $0.5L$, where L is nominal inductance included in the A and B matrices. By changing this nominal inductance the system matrices A, B are changed. For the external load test a 500 g mass was added on the left side of the balance beam. Fig. 10, 12 and 14 show the initial state response when the same initial position is applied. In these figures we can see the close agreement in the transient response to the initial state even if there are parametric variations, which means good robustness of the proposed controller against the parametric variations. Fig. 11, 13 and 15 show the the results of the load test. We loaded a 500 g mass at the first peak and unloaded the same mass at the second peak. From these figures we can see the almost same levitated states and the very small steady state error close to zero under the load, which means effective step disturbance rejections. For the implementation we used the following controller gain matrix and design parameters.

$$S = [15 \;\; 13448.3 \;\; 153.4 \;\; 1.0]$$
$$\rho = 4.0, \; \delta = 0.4 \tag{22}$$

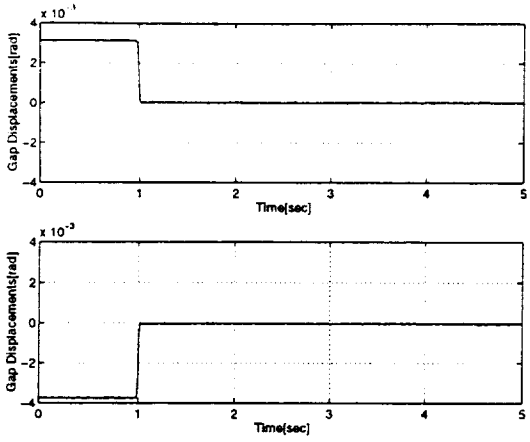

Figure 10: Initial state under the nominal inductance

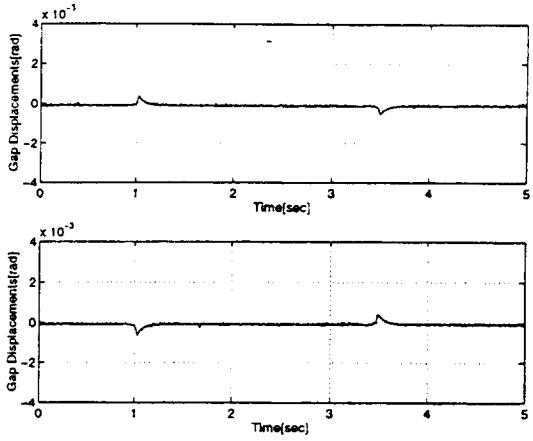

Figure 11: Load 500 g to left side under the nominal inductance

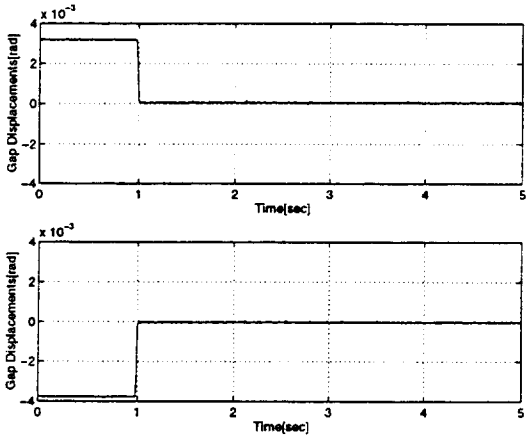

Figure 12: Initial state under two times of the nominal inductance

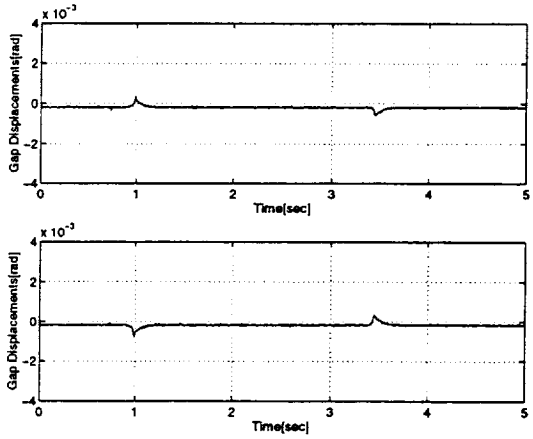

Figure 13: Load 500 g to left side under two times of the nominal inductance

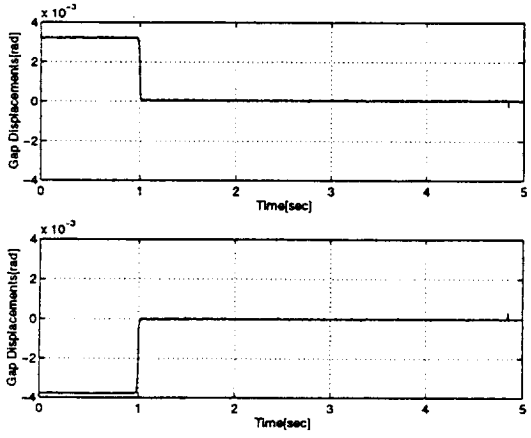

Figure 14: Initial state under 0.5 times of the nominal inductance

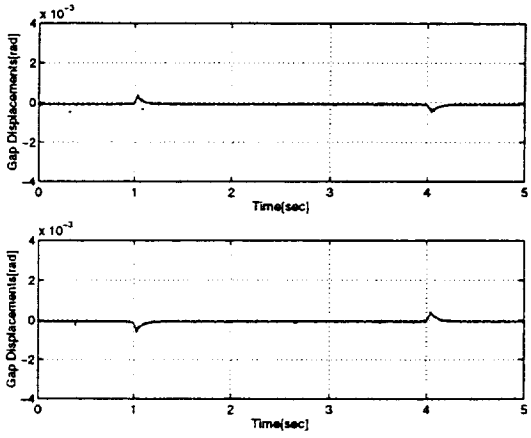

Figure 15: Load 500 g to left side under 0.5 times of the nominal inductance

CONCLUSIONS

This paper presents a method to control the angular displacement of a magnetically suspended balance beam with the parametric variations subject to initial start up conditions and a external step disturbance. To overcome the effect of the parametric variations and to reject the external step disturbance forces we used an integral sliding mode controller. First, we derived the mathematical model of the balance beam including an integral compensator, then we designed the linear and nonlinear control components. Next we showed the insensitivity of the controller response under the parametric variations and the disturbance rejection by simulations. Finally we proved the effectiveness of the integral sliding mode controller by experimentation. This paper does not directly consider plant uncertainties and sinusoidal disturbance forces, hence the next challenging issue is a new control algorithm to consider uncertainties and sinusoidal disturbance force rejection.

REFERENCES

1. P. E. Allaire and A. Sinha, "Robust Sliding Mode Control of a Planar Rigid Rotor System on Magnetic Bearings", *6th International Symposium on Magnetic Bearings, Cambridge, Mass, August 5-7, 1998*

2. S. Ueno, J. H. Lee, P. E. Allaire, Y. Okada, "Sliding Mode Control of Magnetic Bearings:Comparison of Sensed and Self Sensing Performance", *Proceedings on The American Society of Mechanical Engineering(ASME), Indianapolis, Indiana, June 7 - June 10, 1999.*

3. C. Edwards S. K. Spurgeon, "Sliding Mode Control-Theory and Application", *Taylor and Francis Ltd, 1998.*

4. K. Nonami, K. Den, "Sliding Mode Control-Design Theory of Nonlinear Robust Control(Japanese Version)", *Corona, Tokyo, 1994.*

5. S. K. Spurgeon, R. Davies, "A nonlinear control strategy for robust sliding mode performance in the presence of unmatched uncertainty", *INT. J. CONTROL, Vol. 57, No. 5, pp. 1107-1123, 1993.*

6. T. L. Chen, Y. C. Wu, "Integral variable structure control approach for robot manipulators", *IEE Proceedings-D, Vol. 138, No. 2, March, 1992*

7. T. L. Chen, Y. C. Wu, "Design of integral variable structure controller and application to electrohydraulic velocity servosystems", *IEE Proceedings-D, Vol. 138, No. 5, September, 1991*

8. E. Hilton, M. Humphrey, V. Stankovic and P. Allaire, "Real Time Control of a magnetic Bearing Suspension System for Flexible Rotors", *Proceedings of the 5th International Symposium on Magnetic Suspension Technology, Santa Barbara, CA, USA, December 1-3, 1999*